ChemComm



COMMUNICATION

View Article Online



Cite this: Chem. Commun., 2017, **53**. 2483

Received 25th January 2017, Accepted 6th February 2017

DOI: 10.1039/c7cc00727b

rsc.li/chemcomm

Neutral iodotriazole foldamers as tetradentate halogen bonding anion receptors†

Arseni Borissov, Jason Y. C. Lim, Asha Brown, Kirsten E. Christensen, Amber L. Thompson, Martin D. Smith and Paul D. Beer*

Neutral tetradentate halogen bond donor foldamers were synthesised and exhibit enhanced anion affinities over their hydrogen bonding analogues, displaying iodide selectivity over lighter halide, carboxylate and dihydrogen phosphate anions. A foldamer with a chiral (S)-binaphthol motif was demonstrated to distinguish between enantiomers of chiral anions.

Halogen bonding (XB) is the attractive non-covalent interaction between a terminal σ-hole on an electron deficient halogen atom and a Lewis base. 1 Its strength and directionality have led to several applications in materials science and, more recently, in supramolecular chemistry^{2,3} and organocatalysis.⁴ In particular, XB donors have been successfully used in anion receptors for molecular recognition and sensing applications.⁵ Many of these have shown enhanced binding properties over their hydrogen bonding (HB) analogues.6,7

The electron-deficient⁸ 1,2,3-triazole motif has been exploited for anion recognition as an effective C-H hydrogen bond donor when integrated into multidentate macrocycles9 and acyclic foldamers. 10-12 While the related 5-iodotriazole unit has been used as XB donor for anion binding, such XB anion hosts are rare in the literature. 13 No tetradentate XB donor foldamers have been described to date; the closest examples are a tridentate halopyridinium¹⁴ and the use of triazole foldamers as XB acceptor hosts for organohalogens. 15

Herein we sought to apply the potency of XB to enhance the anion affinity of the known triazole-based HB foldamer framework. Thus, XB foldamers with four 5-iodo-1,2,3-triazole XB donors were synthesized (Fig. 1) and their anion binding properties probed in comparison with HB analogues. A few variants were prepared: 1 and 2 contain triethylene glycol (TEG) chains for improved solubility, while in 3 and 4 9-anthrylmethyl termini have

Chemistry Research Laboratory, Department of Chemistry, University of Oxford, Mansfield Road, Oxford, OX1 3TA, UK. E-mail: paul.beer@chem.ox.ac.uk

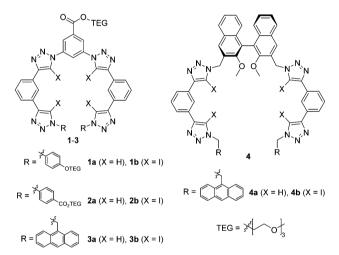


Fig. 1 Structures of the XB and HB anion receptors 1-4

been introduced to provide a fluorescent response. 15,16 System 4 also includes a chiral (S)-binaphthol core in order to investigate XB chiral recognition, which has only previously been observed in a bidentate receptor.¹⁷ Importantly, the XB foldamers exhibited overall stronger anion affinity than their HB analogs with the chiral XB host 4b displaying chiral discrimination with bulky amino acid anions.

XB and HB foldamers 1-4 were synthesized via Cu(1)-catalysed azide-(iodo)alkyne cycloaddition (CuAAC) reactions (Scheme 1) using Cu(MeCN)₄PF₆ in the presence of tris(benzyltriazolylmethyl) amine (TBTA) ligand. For the preparation of 1a and 2a an alternative benzyltriazolylmethylamine (BTA) ligand18 was used as these compounds co-eluted with TBTA during chromatographic purification. As seen in Scheme 1, a terminal azide synthon 5-7 was reacted statistically with an excess of bis-alkyne 8a or 8b to afford an arm fragment 9-11. Two equivalents of 9-11 were then coupled under CuAAC conditions with a bis-azide core synthon 12 or 13 to give the anion receptors 1-4. The cycloadditions proceeded in moderate to high yields of 64-88% for 5H-triazole and 46-85% for 5I-triazole formation (see ESI† for full synthetic details).

[†] Electronic supplementary information (ESI) available: Compound data, crystal data for 3b·NaI, details of anion binding studies. CCDC 1529410. For ESI and crystallographic data in CIF or other electronic format see DOI: 10.1039/ c7cc00727b

Communication ChemComm

$$R = \begin{cases} R - N_3 \\ S - 7 \\ X = H \text{ (8a), I (8b)} \end{cases}$$

$$R = \begin{cases} R = \begin{cases} R - \frac{3^2}{2^2} \\ OTEG \end{cases}$$

$$R = \begin{cases} R - \frac{3^2}{2^2} \\ OTEG \end{cases}$$

$$R = \begin{cases} R - \frac{3^2}{2^2} \\ OTEG \end{cases}$$

$$R = \begin{cases} R - \frac{3^2}{2^2} \\ OTEG \end{cases}$$

$$R = \begin{cases} R - \frac{3^2}{2^2} \\ OTEG \end{cases}$$

$$R = \begin{cases} R - \frac{3^2}{2^2} \\ OTEG \end{cases}$$

$$R = \begin{cases} R - \frac{3^2}{2^2} \\ OTEG \end{cases}$$

$$R = \begin{cases} R - \frac{3^2}{2^2} \\ OTEG \end{cases}$$

$$R = \begin{cases} R - \frac{3^2}{2^2} \\ OTEG \end{cases}$$

$$R = \begin{cases} R - \frac{3^2}{2^2} \\ OTEG \end{cases}$$

$$R = \begin{cases} R - \frac{3^2}{2^2} \\ OTEG \end{cases}$$

$$R = \begin{cases} R - \frac{3^2}{2^2} \\ OTEG \end{cases}$$

$$R = \begin{cases} R - \frac{3^2}{2^2} \\ OTEG \end{cases}$$

$$R = \begin{cases} R - \frac{3^2}{2^2} \\ OTEG \end{cases}$$

$$R = \begin{cases} R - \frac{3^2}{2^2} \\ OTEG \end{cases}$$

$$R = \begin{cases} R - \frac{3^2}{2^2} \\ OTEG \end{cases}$$

$$R = \begin{cases} R - \frac{3^2}{2^2} \\ OTEG \end{cases}$$

$$R = \begin{cases} R - \frac{3^2}{2^2} \\ OTEG \end{cases}$$

$$R = \begin{cases} R - \frac{3^2}{2^2} \\ OTEG \end{cases}$$

$$R = \begin{cases} R - \frac{3^2}{2^2} \\ OTEG \end{cases}$$

$$R = \begin{cases} R - \frac{3^2}{2^2} \\ OTEG \end{cases}$$

$$R = \begin{cases} R - \frac{3^2}{2^2} \\ OTEG \end{cases}$$

$$R = \begin{cases} R - \frac{3^2}{2^2} \\ OTEG \end{cases}$$

$$R = \begin{cases} R - \frac{3^2}{2^2} \\ OTEG \end{cases}$$

$$R = \begin{cases} R - \frac{3^2}{2^2} \\ OTEG \end{cases}$$

$$R = \begin{cases} R - \frac{3^2}{2^2} \\ OTEG \end{cases}$$

$$R = \begin{cases} R - \frac{3^2}{2^2} \\ OTEG \end{cases}$$

$$R = \begin{cases} R - \frac{3^2}{2^2} \\ OTEG \end{cases}$$

$$R = \begin{cases} R - \frac{3^2}{2^2} \\ OTEG \end{cases}$$

$$R = \begin{cases} R - \frac{3^2}{2^2} \\ OTEG \end{cases}$$

$$R = \begin{cases} R - \frac{3^2}{2^2} \\ OTEG \end{cases}$$

$$R = \begin{cases} R - \frac{3^2}{2^2} \\ OTEG \end{cases}$$

$$R = \begin{cases} R - \frac{3^2}{2^2} \\ OTEG \end{cases}$$

$$R = \begin{cases} R - \frac{3^2}{2^2} \\ OTEG \end{cases}$$

$$R = \begin{cases} R - \frac{3^2}{2^2} \\ OTEG \end{cases}$$

$$R = \begin{cases} R - \frac{3^2}{2^2} \\ OTEG \end{cases}$$

$$R = \begin{cases} R - \frac{3^2}{2^2} \\ OTEG \end{cases}$$

$$R = \begin{cases} R - \frac{3^2}{2^2} \\ OTEG \end{cases}$$

$$R = \begin{cases} R - \frac{3^2}{2^2} \\ OTEG \end{cases}$$

$$R = \begin{cases} R - \frac{3^2}{2^2} \\ OTEG \end{cases}$$

$$R = \begin{cases} R - \frac{3^2}{2^2} \\ OTEG \end{cases}$$

$$R = \begin{cases} R - \frac{3^2}{2^2} \\ OTEG \end{cases}$$

$$R = \begin{cases} R - \frac{3^2}{2^2} \\ OTEG \end{cases}$$

$$R = \begin{cases} R - \frac{3^2}{2^2} \\ OTEG \end{cases}$$

$$R = \begin{cases} R - \frac{3^2}{2^2} \\ OTEG \end{cases}$$

$$R = \begin{cases} R - \frac{3^2}{2^2} \\ OTEG \end{cases}$$

$$R = \begin{cases} R - \frac{3^2}{2^2} \\ OTEG \end{cases}$$

$$R = \begin{cases} R - \frac{3^2}{2^2} \\ OTEG \end{cases}$$

$$R = \begin{cases} R - \frac{3^2}{2^2} \\ OTEG \end{cases}$$

$$R = \begin{cases} R - \frac{3^2}{2^2} \\ OTEG \end{cases}$$

$$R = \begin{cases} R - \frac{3^2}{2^2} \\ OTEG \end{cases}$$

$$R = \begin{cases} R - \frac{3^2}{2^2} \\ OTEG \end{cases}$$

$$R = \begin{cases} R - \frac{3^2}{2^2} \\ OTEG \end{cases}$$

$$R = \begin{cases} R - \frac{3^2}{2^2} \\ OTEG \end{cases}$$

$$R = \begin{cases} R - \frac{3^2}{2^2} \\ OTEG \end{cases}$$

$$R = \begin{cases} R - \frac{3^2}{2^2} \\ OTEG \end{cases}$$

$$R = \begin{cases} R - \frac{3^2}{2^2} \\ OTEG \end{cases}$$

$$R = \begin{cases} R - \frac{3^2}{2^2} \\ OTEG \end{cases}$$

$$R = \begin{cases} R - \frac{3^2}{2^2} \\ OTEG \end{cases}$$

$$R = \begin{cases} R - \frac{3^2}{2^2} \\ OTEG \end{cases}$$

$$R = \begin{cases} R$$

Scheme 1 Synthesis of the anion receptors 1-4. Reaction conditions: (i) 0.05 eg. Cu(MeCN)₄PF₆, 0.05 eg. TBTA or BTA, 0.1 eg. DIPEA, DCM, rt; (ii) 0.1 eq. Cu(MeCN)₄PF₆, 0.1 eq. TBTA, THF, rt, darkness.

The anion binding properties of 1-4 were studied by ¹H NMR titrations by adding increasing amounts of different anions as tetrabutylammonium (TBA) salts and monitoring changes in ¹H NMR spectra. For the HB receptors 1a-4a large downfield shifts $(\Delta \delta)$ of up to 2 ppm were observed for the triazole protons H_A and H_B ; while smaller $\Delta\delta$ of 0.4-0.5 ppm occurred for the phenylene protons H_C and H_E (Fig. 2). This is consistent with the known binding mode of tetradentate triazole HB receptors¹⁰ wherein the triazole protons and the phenylene ortho protons all contribute to guest complexation. Binding isotherms were obtained by monitoring HA signals and 1:1 stoichiometric association constants calculated using WinEQNMR2 software. 19

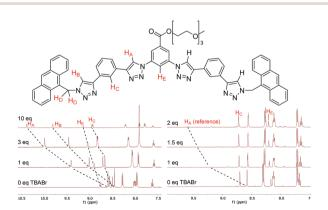


Fig. 2 Top: Labeling of protons monitored in ¹H NMR anion binding studies (consistent across 1-4). Bottom left: Partial ¹H NMR spectra of 2a titrated with TBABr. Bottom right: Partial ¹H NMR spectra of a competition experiment where 2b with 5 mol% of 2a as reference is titrated with TBABr (500 MHz, CDCl₃, 298 K).

In the case of XB foldamers 1b-4b only small downfield perturbations $\Delta\delta$ of 0.03-0.2 ppm were observed for the *ortho* phenylene protons H_C and H_E. This is most likely due to the large size of the receptors' iodine atoms binding the guest anion at a significant distance from these protons (vide infra). Upfield shifts of similar magnitude were also observed for the aromatic and methylene protons in the terminal groups. Due to very small $\Delta\delta$ values reliable association constants could not be obtained for **1b–3b** using the standard ¹H NMR titration protocol. Therefore, 1b-3b were instead analysed using a host-host competition binding method similar to approaches previously employed to study alkali metal complexation with crown ethers.²⁰ In a typical experiment a small amount (5 mol%) of HB receptor 2a was added to the solution of a XB compound 1b-3b as a reference. Changes of the reference compound HA signals upon anion addition were then monitored (Fig. 2), which enabled reliable association constant data to be determined for 1b-3b (see ESI† for full details). While 4b could not be analysed by this technique due to the lack of a suitable reference compound, it exhibited sufficient magnitude of downfield shifts in its H_C protons to provide good quality data using a standard ¹H NMR titration protocol.

As shown by the anion association constants for 1-4 given in Table 1, the XB foldamers 1b-4b were found to be stronger halide and oxoanion receptors than their HB analogs. This difference is especially prominent in systems 3 and 4. This is because the XB receptors rely predominantly on the iodotriazole XB donors for anion affinity, whereas their HB analogues benefit in part from secondary HB donors at the phenylene rings next to the triazoles. 10,11 Deletion of these binding elements as in 3a and 4a leads to fewer convergent HB interactions and consequently a large loss of anion affinity. The XB receptors, on the other hand, are tolerant to these modifications. Thus, the anthryl-terminated 3b displayed affinity for Br and I that was two orders of magnitude stronger than of 3a. Likewise, XB receptor 4b exhibited notable K_a values of up to 500 M⁻¹ in 1:1 $CDCl_3$ /acetone- d_6 , while **4a** displayed almost no binding (too weak to be quantified).

Table 1 Association constants^a K_a [M⁻¹] for **1-4** with halides and oxvanions^a

	Cl^-	Br^-	\mathbf{I}^-	$\mathrm{H_2PO_4}^-$	AcO^-	L-Tartrate
1a	232 (3)	356 (10)	427 (9)	1244 (83)	69 (1)	331 (3)
1b	433 (44)	600 (46)	1202 (87)	-b	320 (57)	281 (27)
2a	466 (18)	740 (29)	960 (46)	2751 (92)	174 (4)	672 (9)
2b	592 (59)	902 (76)	2131 (142)	b	504 (88)	549 (41)
3a	20 (2)	15 (1)	24 (1)	87 $(11)^c$	d	64 (1)
3b	742 (65)	1235 (79)	2712 (187)	$493 (80)^e$	753 (116)	585 (43)
4a	d	d	d	37 (3)	d	d
4b	335 (14)	384 (28)	511 (94)	207 (4)	165 (9)	445 (16)

^a 1:1 binding stoichiometry. All anions introduced as TBA salts; 1-3 studied in $CDCl_3$; 4 in 1:1 $CDCl_3$ /acetone- d_6 (500 MHz, 298 K); [receptor] = 1.5 mM. Unless stated otherwise, K_a for 1a-4a were derived from H_A; for 4b from H_C; for 1b-3b from H_A of the reference compound 2a using the competition method. Uncertainties are given in parentheses. b Could not be determined as HB foldamers are too strong H₂PO₄ binders to be used as reference compounds. ^c Derived from H_E. ^d Too weak to be quantified. ^e Derived from H_C using the standard ¹H NMR titration method.

ChemComm Communication

Comparing the XB foldamers, the anion binding strength is in the order 3b > 2b > 1b > 4b. This indicates that the wider spacing of the bis-iodotriazole arms in 4b leads to less effective alignment of its XB donors with halides and carboxylates. As expected, 2b exhibited 1.5-2 times higher K_a values than **1b** due to its more electron-withdrawing termini, which is also observed in the HB analogues 1a and 2a.

The XB receptors displayed the order of selectivity I > $Br^- > Cl^- \approx AcO^- \approx H_2PO_4^-$, which suggests better hostguest size complementarity with larger halides. Additionally, neutral XB donors 1-4 do not display charge assistance that might favour binding of small, hard anions in cationic hosts. Interestingly, tartrate²⁻ > AcO⁻ selectivity was observed in HB receptors 1a-3a and XB receptor 4b but not in 1b-3b. This may indicate that with 1b-3b, the anion binding cavity is too small to simultaneously bind both anionic groups in a dicarboxylate due to the large size of the four convergent iodine atoms. Increased spacing between the bis(iodotriazole) arms in 4b allows both carboxylate groups to be bound and induces dicarboxylate selectivity. This is also seen in HB analogues which have a less crowded anion binding site.

Single crystals of 3b·NaI suitable for X-ray structural analysis were obtained by combining 3b and excess NaI in 6:4 CHCl₃/acetone.‡ The structure (Fig. 3) shows the XB host encapsulating I via four linear halogen bonds [C-I···I⁻ distances: 3.484(1)-3.574(2) Å $(88-90\% \text{ of } \Sigma r_{\text{vdW}})^{21} \text{ C-I} \cdots \text{I}^- \text{ angles: } 165.7(3)-178.3(3)^{\circ}]. \text{ Due to the}$ large size of the four iodine XB donor atoms the wrapping of the foldamer around the guest anion is less tight than in the analogous HB systems.²² The iodotriazoles are tilted by 29-54° relative to the neighbouring phenylene rings and the I guest is situated 3.01 Å above the mean plane of the foldamer backbone. The Na⁺ countercation is complexed by the triethylene glycol chain, with an acetone solvate molecule and a triazole N³ atom from an adjacent molecule completing its coordination sphere.

The XB receptors 3b and 4b displayed an intense fluorescence in 375-525 nm region arising from the emission of anthracene termini (Fig. 4). In 3b a large increase in emission intensity, without changes in wavelength, occurred upon addition of TBABr.

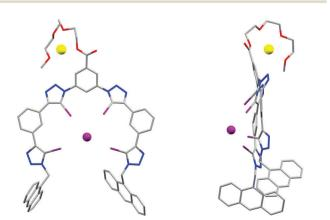


Fig. 3 X-ray crystal structure of 3b·Nal showing the face-on (left) and side-on (right) view, visualising the folding of the receptor in a capped configuration.

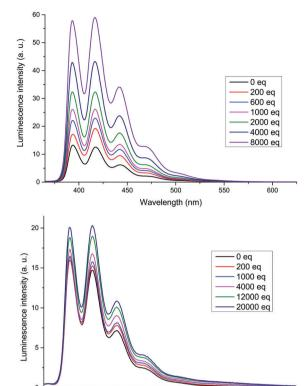


Fig. 4 Emission spectra of 3b (top) and 4b (bottom) titrated with TBABr. Host concentration: 1 μM in CHCl₃ (3b) or 1:1 CHCl₃/acetone **(4b)**, $\lambda_{ex} = 350 \text{ nm}$.

Wavelength (nm)

400

A small increase was also observed for 4b; the most significant change occurred in the emission peak at 420 nm for both receptors. The overall increase in fluorescence intensity upon anion binding is most probably due to conformational rigidification of the receptor which suppresses non-radiative decay pathways. Thus, the larger fluorescence enhancement in 3b is likely due to 3b being less disordered in its bound state than 4b. As seen in the solid state structure of 3b·NaI, the anthracene termini are too far from each other for effective intramolecular π-stacking which accounts for the absence of excimer emission.23

Table 2 Association constants K_a [M⁻¹] for **4b** with enantiomers of chiral carboxylates^a

	$K_a^{\ b}$	$K_{ m D}/K_{ m L}$
L-Boc-Ala	336 (23)	0.79 (0.17)
D-Boc-Ala	265 (52)	` ,
L-Boc-Leu	287 (38)	1.52 (0.21)
D-Boc-Leu	436 (21)	, ,
L-Boc-Trp	200 (14)	1.69 (0.12)
D-Boc-Trp	337 (4)	, ,
L-Tartrate	725 (6)	1.29 (0.04)
D-Tartrate	932 (28)	` ,
L-Glutamate	1483 (220)	0.92 (0.15)
D-Glutamate	1363 (99)	` ,

^a All anions were introduced as TBA salts. All titrations were undertaken in 1:1 CDCl $_3$ /acetone- d_6 (500 MHz, 298 K). Uncertainties are given in parentheses. b Determined from titration data monitoring H_D.

Communication ChemComm

Chiral XB **4b** receptor was titrated with both enantiomers of Boc-Ala, Boc-Leu, Boc-Trp, Glu and tartrate as TBA salts. The association constant values shown in Table 2 reveal varying degrees of chiral discrimination were observed with different anions. The greatest difference in affinity was observed for tryptophan ($K_{\rm D}/K_{\rm L}=1.69$), followed by leucine and alanine, which correlates with the steric bulk of the amino acid residue. In the case of the dicarboxylate guests, a modest degree of discrimination was seen for tartrate while no difference was observed for glutamate. This is once again consistent with the steric factors of guest anions.

In summary a series of novel neutral tetrakis(5-iodo-1,2,3-triazole) foldamers **1b–4b** was prepared and evaluated as halogen bonding anion receptors. Importantly, compared to their HB analogues **1a–4a**, the XB foldamers showed enhanced anion affinities, with a general preference for binding heavier halides over oxoanions. The advantage of XB for anion binding is especially evident in **3b** and **4b** where the HB analogues **3a** and **4a** displayed very weak affinities due to the deletion of secondary HB donors, while the XB foldamers **3b** and **4b** remained effective as anion receptors. The incorporation of anthracene and chiral BINOL groups into the XB foldamer structure design demonstrated fluorescent anion sensing and chiral discrimination capabilities which are currently under further investigation.

We thank the EPSRC centre for Doctoral Training in Synthesis for Biology and Medicine (EP/L015838/1), the Agency for Science, Technology and Research (A*STAR), Singapore, and the European Research Council (FP7/2007–2014, ERC Advanced Grant Agreement No. 267426) for financial support, Diamond Light Source for an award of beamtime on I19 (MT13639) and the beamline scientists for technical support.

Notes and references

‡ Single crystal diffraction data were collected at 100(2) K using a custom-built Crystal Logic diffractometer and synchrotron radiation ($\lambda=0.6889$ Å) at Diamond Light Source, beamline I19.²⁴ Unit cell parameter determination and data reduction were carried out using CrysAlisPro. The structures were solved by charge-flipping with SUPERFLIP²⁵ and refined by full matrix least squares on F^2 using CRYSTALS.^{26–28} Full refinement details are given in the ESI.† Single crystal data: $C_{64}H_{48}I_5N_{12}NaO_5Zn\cdot4(C_3H_6O)$, $M_r=1954.99$; triclinic, $P\bar{1}$; a=14.3220(4) Å, b=17.7665(5) Å, c=17.7815(5) Å, $\alpha=113.335(2)^\circ$, $\beta=100.303(2)^\circ$, $\gamma=93.903(2)^\circ$, V=4038.8(2) ų; data, restraints,

parameters: 11420/955/928; $R_{\rm int}$ = 0.195, final R_1 = 0.100, w R_2 = 0.281 (F^2 ; [$I > 2\sigma(I)$]); $\Delta\rho_{\rm min,max}$ = -3.28, +2.38 e Å $^{-3}$. CCDC 1529410.

- 1 G. Cavallo, P. Metrangolo, R. Milani, T. Pilati, A. Priimagi, G. Resnati and G. Terraneo, *Chem. Rev.*, 2016, **116**, 2478–2601.
- 2 P. Metrangolo, F. Meyer, T. Pilati, G. Resnati and G. Terraneo, Angew. Chem., Int. Ed., 2008, 47, 6114–6127.
- 3 L. C. Gilday, S. W. Robinson, T. A. Barendt, M. J. Langton, B. R. Mullaney and P. D. Beer, *Chem. Rev.*, 2015, 115, 7118–7195.
- 4 S. Schindler and S. M. Huber, Halogen Bonding Ii: Impact on Materials Chemistry and Life Sciences, 2015, vol. 359, pp. 167-203.
- 5 T. M. Beale, M. G. Chudzinski, M. G. Sarwar and M. S. Taylor, *Chem. Soc. Rev.*, 2013, 42, 1667–1680.
- 6 N. L. Kilah, M. D. Wise, C. J. Serpell, A. L. Thompson, N. G. White, K. E. Christensen and P. D. Beer, *J. Am. Chem. Soc.*, 2010, 132, 11893–11895.
- 7 R. Tepper, B. Schulze, M. Jager, C. Friebe, D. H. Scharf, H. Gorls and U. S. Schubert, J. Org. Chem., 2015, 80, 3139–3150.
- 8 B. Schulze and U. S. Schubert, *Chem. Soc. Rev.*, 2014, 43, 2522–2571. 9 Y. L. Li and A. H. Flood, *J. Am. Chem. Soc.*, 2008, **130**, 12111–12122.
- 10 H. Juwarker, J. M. Lenhardt, D. M. Pham and S. L. Craig, Angew. Chem., Int. Ed., 2008, 47, 3740–3743.
- 11 H. Juwarker, J. M. Lenhardt, J. C. Castillo, E. Zhao, S. Krishnamurthy, R. M. Jamiolkowski, K. H. Kim and S. L. Craig, *J. Org. Chem.*, 2009, 74, 8924–8934.
- 12 J. Shang, W. Zhao, X. Li, Y. Wang and H. Jiang, Chem. Commun., 2016, 52, 4505–4508.
- 13 A. Brown and P. D. Beer, Chem. Commun., 2016, 52, 8645-8658.
- 14 C. J. Massena, N. B. Wageling, D. A. Decato, E. Martin Rodriguez, A. M. Rose and O. B. Berryman, Angew. Chem., 2016, 55, 12398–12402.
- L. Y. You, S. G. Chen, X. Zhao, Y. Liu, W. X. Lan, Y. Zhang, H. J. Lu,
 C. Y. Cao and Z. T. Li, Angew. Chem., Int. Ed., 2012, 51, 1657–1661.
- 16 F. Zapata, A. Caballero, P. Molina, I. Alkorta and J. Elguero, J. Org. Chem., 2014, 79, 6959–6969.
- 17 J. Y. C. Lim, I. Marques, L. Ferreira, V. Felix and P. D. Beer, *Chem. Commun.*, 2016, 52, 5527–5530.
- 18 T. R. Chan, R. Hilgraf, K. B. Sharpless and V. V. Fokin, Org. Lett., 2004, 6, 2853–2855.
- 19 M. J. Hynes, J. Chem. Soc., Dalton Trans., 1993, 311-312.
- 20 J. M. Daniel, S. D. Friess, S. Rajagopalan, S. Wendt and R. Zenobi, Int. J. Mass Spectrom., 2002, 216, 1–27.
- 21 A. Bondi, J. Phys. Chem., 1964, 68, 441-451.
- 22 Y. R. Hua, Y. Liu, C. H. Chen and A. H. Flood, J. Am. Chem. Soc., 2013, 135, 14401–14412.
- 23 K. Ghosh, A. R. Sarkar, A. Ghorai and U. Ghosh, New J. Chem., 2012, 36, 1231–1245.
- 24 H. Nowell, S. A. Barnett, K. E. Christensen, S. J. Teat and D. R. Allan, *J. Synchrotron Radiat.*, 2012, **19**, 435–441.
- 25 L. Palatinus and G. Chapuis, J. Appl. Crystallogr., 2007, 40, 786-790.
- 26 P. W. Betteridge, J. R. Carruthers, R. I. Cooper, K. Prout and D. J. Watkin, J. Appl. Crystallogr., 2003, 36, 1487.
- 27 P. Parois, R. I. Cooper and A. L. Thompson, Chem. Cent. J., 2015, 9, 30.
- 28 R. I. Cooper, A. L. Thompson and D. J. Watkin, J. Appl. Crystallogr., 2010, 43, 1100–1107.